Supplementary Information for

An unanticipated architecture of the 750 kD $\alpha_6\beta_6$ holoenzyme of 3-methylcrotonyl-CoA carboxylase

Christine S. Huang,[1] Peng Ge,[2] Z. Hong Zhou,[2] Liang Tong[1]

[1]Department of Biological Sciences
Columbia University
New York, NY 10027, USA

[2]Department of Microbiology, Immunology and Molecular Genetics
California NanoSystems Institute
University of California, Los Angeles
Los Angeles, CA 90095, USA

Correspondence information for Liang Tong

Phone: (212) 854-5203, FAX: (212) 865-8246

E-mail: ltong@columbia.edu

Supplementary text

Distinct domain organization of MCCβ compared to PCCβ

The primary reason for the swapping of the positions of the N and C domains in PaMCCβ when compared to PCCβ is that the linker between the two domains runs in the opposite direction, and consequently connects the N domain to a different C domain in MCC compared to PCC (Supplementary Fig. 3). The neighboring linkers in the PaMCC structure come very close to each other in the hexamer (Supplementary Fig. 3), and therefore only a small change is needed to switch the connectivity as observed in PaMCCβ to that in PCCβ, and this change in connectivity has only minor effects on the overall structure of the hexamer. The two linkers have essentially the same length, with that in PCCβ containing one extra residue compared to MCCβ (Supplementary Fig. 2).

Therefore, the swapping of the positions of the N and C domains in MCCβ compared to PCCβ is due to a different connectivity between the two domains, and is not due to a swap of these domains in the primary sequences of the two proteins. The N-terminal half of MCCβ still shares stronger sequence conservation with the N-terminal half of PCCβ. The different connectivity does lead to a different position of the C domain relative to the N domain in MCCβ compared to PCCβ (Supplementary Fig. 3).

In addition, PaMCCβ has a long segment (including a long helix) at the N-terminus, which actually lies over the C domain (Fig. 1e). This interaction is unique to PaMCCβ when compared to PCCβ (which has a much shorter segment/helix at the N-terminus), and contributes approximately 900 $Å^2$ to the buried surface area. Therefore, the buried surface area between the N and C domains of each subunit (~950 $Å^2$) in PCCβ is comparable to that between neighboring subunits in each layer of the hexamer (~900 $Å^2$). In contrast, the buried surface area between neighboring subunits in the PaMCCβ hexamer is ~900 $Å^2$, comparable to PCCβ, while that between the N and C domains of each subunit is ~2000 $Å^2$. Therefore, this long N-terminal segment may be important for stabilizing the domain organization observed in PaMCCβ. In fact, this segment may be the determining factor for this swapped domain organization. It is also present in GCDα (Supplementary Fig. 4), and sequence analysis suggests that it may be present in GCC as well (Supplementary Fig. 18). On the other hand, the linker between the N and C domains is roughly the same length in all of these enzymes (including PCC and ACC) and is poorly conserved in sequence, and therefore is unlikely the driving force for the difference in connectivity between MCC and PCC.

The N and C domains of the β subunit have the same backbone fold. The pseudo symmetry operation relating the two domains is a rotation of approximately 60°, along the three-fold axis of the β_6 hexamer. Therefore, the β_6 hexamers of MCC and PCC have pseudo six-fold symmetry. The swapping of the N and C domains in MCC follows this pseudo symmetry, and does not lead to a dramatic change in the overall shape of the hexamer. In fact, the β_6 hexamer of MCC can be superimposed onto that of PCC by a 60° rotation around the 3-fold axis of the hexamer, giving a rms distance of 1.6 Å for 2,600 equivalent Cα atoms. This 60° rotation can also be visualized by the difference in the orientation of the triangle-shaped central hole in the structures of MCC (Fig. 2b) compared to PCC (Fig. 2d).

The molecular replacement solution using the structure of PCCβ as the model also reflected this pseudo symmetry. The solution matched the N and C domains of PCCβ to the neighboring N and C domains of two separate (crystallographically-related) PaMCCβ subunits.

A possible difference in the architecture of MCC holoenzyme compared to PCC due to the swapping of the N and C domain positions in the β subunit

In the PCC holoenzyme, the α subunit, through its BT domain, primarily contacts the N domain of the β subunit [1]. The swapping of the N and C domains in PaMCCβ suggests that the positions of the α subunit are likely different in the MCC holoenzyme. To maintain contacts between the α subunit (BT domain) and the N domain of the β subunit, one solution would be to rotate the α subunits by 60° relative to their positions in PCC, following the pseudo six-fold symmetry of the β_6 hexamer.

This 60° rotation of the α subunit relative to its position in PCC is observed in the structure of the PaMCC holoenzyme (compare Figs. 2b and 2d), so that the α subunit remains primarily in contact with the N domain of the β subunit. However, significant additional differences are observed in the position of the α subunits, such that the overall shape of the MCC holoenzyme is strikingly different from that of PCC.

Substrate selectivity of MCC

The structural and sequence analyses suggest a correlation between the swapped domain organization (for MCC, GCDα, and GCC) and the carboxylation on the γ carbon of the substrate. While the exact mechanism for this correlation will require further studies, it is possible that a swapped organization helps to position the CoA and/or biotin substrate correctly in the active site for catalysis to happen on the γ carbon. In addition, there are conformational differences (both structural re-arrangements and side-chain variations) in the active site region between PCCβ and MCCβ, which allows the latter to accommodate the larger methylcrotonyl-CoA substrate. Modeling this substrate into the active site of PCCβ shows that there may be steric clashes between this substrate and the active site, especially the Tyr176 residue. The equivalent residue in MCCβ, Phe191, has a different position for its side chain and avoids the steric clash, due to differences in the main-chain conformation in this region of the two structures. Therefore, the swapped domain organization and local structural differences and sequence variations all contribute to the substrate selectivity of MCC.

Overall structures of the PaMCC holoenzyme

An αβ protomer is in the asymmetric unit of the PaMCC free enzyme crystal. The $\alpha_6\beta_6$ dodecamer is generated by the crystallographic symmetry (*R*32). The BCCP domain of the α subunit is disordered in this crystal, and weak electron density is observed for the B domain of BC, in an open conformation (Supplementary Fig. 5). In the β subunit, several segments of the protein near the active site, including residues 180-189 (β7-α4 loop in the N domain, Supplementary Fig. 2), 244-266 (α6-α7), 407-416 (β7-α4 loop in the C domain), 444-450 (β9-α5), and 470-514 (α6-α6A, which forms a large protrusion on the surface of the β subunit, Fig. 2a), are disordered in the free enzyme (Supplementary Fig. 5). This is in contrast to the structure of PaMCCβ alone, where these

residues are well ordered (Fig. 1e). The free enzyme structure of a better fit to the EM density (Fig. 2e), which was obtained in the absence of CoA.

An entire $\alpha_6\beta_6$ holoenzyme is located in the crystallographic asymmetric unit of the CoA complex of PaMCC. The six molecules of each subunit have essentially the same conformation, with rms distance of approximately 0.25 Å for their equivalent Cα atoms (non-crystallographic symmetry restraint was applied during refinement). The B domain of BC is ordered in four of the six α subunits, in an open conformation (Fig. 2a). BCCP is ordered in only one of the α subunits, and is located in the active site of MCCβ (Fig. 2a). Weak electron density for biotin and the lysine residue it is covalently linked to was observed in another subunit.

The overall structures of the free enzyme and the CoA complex of PaMCC holoenzyme are similar. The rms distance among 2,566 equivalent Cα atoms of the β subunits of the two structures is 0.9 Å. On the other hand, this overlay of the β subunits revealed a change in the position of the α subunits in the two structures, which corresponds to a rotation of ~6°, mostly along the 3-fold axis of the holoenzyme (Supplementary Fig. 5).

The rms distance for equivalent Cα atoms between the structure of PaMCCβ alone and that in either of the two holoenzymes is ~0.8 Å. Residues at the interface with the α subunit assume the same conformation in the structure of MCCβ alone, suggesting that the β subunit does not undergo a large conformational change upon the formation of the holoenzyme. In contrast, large structural differences are observed for helices α6 and α6A near the active site of the β subunit in the CoA complex.

There is no direct contact between the BC domain in the α subunit and the β subunit in the PaMCC holoenzyme, with the two entities separated by nearly 20 Å (Fig. 2a), whereas there is some contact between BC and the β subunit in PCC (Fig. 2c) [1]. The BT domain is the bridge between BC and the β subunit in PaMCC (Figs. 2a, 4c). However, in contrast to BC, there is no contact among the BT domains in PaMCC, which leaves a large cavity between BC and the β subunit (Fig. 2a).

The BT domain of human MCC

The BT domain of PaMCC lacks the third strand (β24) and the fourth strand (β25) is much shorter compared to the eight-stranded β-barrel in the BT domain of PCC (Fig. 3a). Instead, the second and the fourth strands are connected directly by a short linker. Interestingly, PaMCC contains a deletion of 14 residues in this region as compared to HsMCC, and secondary structure prediction suggests that these additional residues in HsMCC likely can form the third strand and extend the length of the fourth strand (Supplementary Fig. 1). Therefore, it is probable that the BT domain of HsMCC actually contains an eight-stranded β-barrel, which would be equivalent to that in PCC. In fact, sequence comparisons suggest that this deletion may be unique to the *Pseudomonas* organisms, while most other MCCs are similar to HsMCC. Therefore, the BT domain of most MCC holoenzymes is likely to have an eight-stranded β-barrel.

The third and fourth strands are not located in the subunit interface in PaMCC (Fig. 3b) and PCC [1], and therefore their absence in PaMCC is unlikely to have caused a large difference in the overall structure of the BT domain or the organization of the dodecamer.

While the overall structure of the BT domain of PaMCC is generally similar to that of PCC, the detailed positions of the β-strands and the central helix are rather different (Fig. 3a). In addition, the central helix in the BT domain of PaMCC is much shorter compared to that in PCC.

These detailed structural differences between the BT domains of MCC and PCC, especially their hooks, may be the basis for the different locations of the BC domains in the two holoenzymes, such that PCC has monomeric BC domains while MCC has trimeric BC domains.

BT domain interactions in the PaMCC holoenzyme

The hook and the first β-strand (β22) of the BT domain have the most contacts with the β subunit (Fig. 3b). The hook interacts with residues at the interface between the N and C domains of the β subunit (Fig. 3c). Residues in the hook that make the most contribution to surface area burial include two Trp residues (Trp537 and Trp543) and two Arg residues (Arg525 and Arg544). In addition, Asp535 in the hook has ion-pair interactions with Lys298 in the β subunit, which is in the linker between the N and C domains.

Residues 633-636 (αW helix of the BT domain) are located near the α8 helix in the N domain of the β subunit, as well as the N-terminus of a neighboring β subunit.

Direct interactions between the BT domain and the BC domain of a neighboring α subunit are mediated by the N-terminal end of the sixth strand (β27, Fig. 3b). This interface is primarily mediated by hydrogen-bonding among main-chain atoms, forming the anti-parallel β-sheet. There is little side chain contact in this interface. The β26-β27 hairpin has large structural differences compared to that in the BT domain of PCC (Fig. 3a).

Binding mode of CoA to the PaMCC holoenzyme

Methylcrotonyl-CoA was included in the crystallization solution, but only CoA was observed based on the electron density (Supplementary Fig. 13), suggesting that the CoA ester may have been hydrolyzed during crystallization. The conformation of CoA, especially the 3'-phospho-ADP portion, is different from that bound to GCDα [2], and is actually more similar to that bound to the CT domain of yeast acetyl-CoA carboxylase (ACC) [3].

The adenine base is sandwiched between the side chain of Thr144 (strand β5 in the N domain of β6) and those of Leu482 and Val485 (helix α6 in the C domain of β3, Supplementary Fig. 14). The phosphate groups of CoA are recognized by the side chains of Arg74 and Arg78 (helix α1), and Lys141 (β4-β5 loop) in the N domain.

A large conformational change for helices α6 and α6A in the C domain is associated with CoA binding, which rotate by roughly 25° to move closer to the adenine (Supplementary Fig. 15). These two helices are also involved in crystal packing in both the PaMCCβ and the holoenzyme crystals. In GCDα, helix α6 rotates by 13° upon the binding of crotonyl-CoA [2]. A smaller conformational change for helix α1, which contains the two Arg side chains that interact with the phosphates of CoA, is also observed (Supplementary Fig. 15).

Based on our structure of the CoA complex and the conformation of crotonyl-CoA bound to GCDα [2], we built a model for the binding mode of methylcrotonyl-CoA to the

active site of PaMCC (Fig. 4b, Supplementary Fig. 14). This ternary complex provides significant molecular insights into the catalytic mechanism of MCC and biotin carboxylases in general. It is expected that the N1' atom of biotin, in its enolate form, can extract a proton from the γ carbon of methylcrotonyl-CoA [4]. Our structure shows that the enolate oxygen atom of biotin is stabilized by an oxyanion hole consisting of the main-chain amides of Phe407 (in strand β7) and Gly448 (at the N-terminus of helix α5) in the C-domain of one β subunit (Supplementary Fig. 14). Therefore, the oxyanion also has favorable interactions with the dipole of helix α5. Upon proton extraction, the methylcrotonyl group also enolizes, and that oxyanion is stabilized by the main-chain amides of Ala176 (in strand β7) and Gly219 (at the N-terminus of helix α5) in the N-domain of another β subunit (Supplementary Fig. 14). The two oxyanion holes employ equivalent residues in the N and C domains of the β subunit. This mechanism is similar to that proposed for GCDα [5].

Methylcrotonyl-CoA has a second, non-reactive γ carbon (Fig. 1b), which is absent in crotonyl-CoA. In the model, this γ carbon is located in a pocket formed by the side chains of Phe191 (helix α4), Ala176 (β7), and the main chain of Gly219 (α5). Our kinetic experiments showed that the activity of PaMCC towards crotonyl-CoA is roughly 90% of that towards methylcrotonyl-CoA, indicating that the enzyme is not selective with respective to these two substrates. In contrast, PaMCC is essentially inactive towards propionyl-CoA, with less than 1% of the activity compared to methylcrotonyl-CoA.

Binding mode of BCCP

The BCCP domain contacts the C domain of one β subunit (β3) through its 679-AMKM-682 biotinylation sequence as well as residues Met653-Asn654 (Supplementary Fig. 17). There is a hydrogen bond between the main-chain amide of residue Glu683 and the carbonyl group of Lys326. In addition, residues Ala250-Thr251, at the end of helix α6 of the N domain of a second β subunit (β6), also have interactions with the BCCP domain (Supplementary Fig. 17). Two residues in this interface, Ile375 (Val in HsMCC) and Asn403, are sites of disease-causing mutations, which may affect the positioning of BCCP in the CT active site for catalysis.

The interface between BCCP and the β subunit is rather rich in Met residues, with Met653, Met680 and Met682 from BCCP, and Met408 and Met473 from the β subunit (Supplementary Fig. 17).

Disease-causing mutations

Of the disease-causing mutations in the α subunit, R385S disrupts the Arg side chain that is expected to stabilize the biotin enolate during BC catalysis, based on studies with the BC subunit of *E. coli* ACC (Supplementary Fig. 16) [6]. The E134K mutation may disturb the interaction with Arg339, which recognizes the bicarbonate substrate.

The I460M mutation affects a residue that is located in the interface between the BC and BT domains of the same subunit (Supplementary Fig. 16). It may disturb the position of the BC domain relative to the rest of the holoenzyme.

The S535F mutation in the hook of the BT domain may disrupt the interactions between the α and β subunits (Supplementary Fig. 12). The Ser side chain is located in a small pocket in the α-β interface, and the S535F mutation may lead to large conformational re-arrangements in this region of the interface. The D532H mutation in

the BT domain (as well as the I437V mutation in the β subunit) primarily affects splicing in humans (Table S2) [7], although it may also affect the holoenzyme (Supplementary Fig. 12).

Of the disease-causing mutations in the β subunit, A218T may disrupt binding of methylcrotonyl-CoA or biotin (or both), being centrally located between these two substrates (Fig. 4b). The H190Y/R, R193C/H and A456V mutations form a cluster and are located near the binding site for the methylcrotonyl group. The S173L mutation is located near the binding site for the adenine base of CoA.

Several of the disease-causing mutations in the β subunit may disturb interactions with the BT domain. These include E99Q, S101F and H282R. Two other mutations are located in the interface with BCCP, V375F and N403T.

Table 1.

Summary of crystallographic information

Structure	**PaMCCβ Free enzyme**	**PaMCC Free enzyme**	**PaMCC CoA complex**
Space Group	*R*32	*R*32	$P2_1$
Unit cell parameters	*a*=*b*=192.4 Å, *c*=136.8 Å	*a*=*b*=158.9 Å, *c*=312.0 Å	*a*=131.5 Å, *b*=255.3 Å, *c*=152.7 Å β=95.7 °
Resolution range (Å) [1]	30–1.5 (1.55–1.5)	50–2.9 (3.0–2.9)	50–3.5 (3.63–3.5)
Number of observations	508,819	121,925	363,300
Number of reflections	141,517	31,522	104,480
Completeness (%)	92 (73)	93 (82)	83 (61)
R_{merge} (%)	8.9 (35.9)	5.8 (38.8)	12.0 (45.1)
I/σI	10.8 (2.3)	16.0 (2.4)	8.3 (1.7)
Redundancy	3.4 (2.6)	3.6 (3.4)	3.1 (2.4)
R factor (%)	16.6 (32.8)	20.9 (32.4)	23.4 (39.6)
Free *R* factor (%)	18.3 (31.8)	26.9 (35.4)	29.2 (42.5)
rms deviation in bond lengths (Å)	0.017	0.011	0.014
rms deviation in bond angles (°)	1.7	1.7	1.8
Number of protein atoms	4,046	7,636	49,946
Number of waters	970	0	0
Ramachandran plot (% of residues)			
Most favored region	92.3	78.9	75.6
Additional allowed region	7.5	17.8	21.6
Generously allowed region	0.2	2.7	2.3
Disallowed region	0	0.6	0.5

1. The numbers in parentheses are for the highest resolution shell.

Table 2.
Missense mutations in HsMCC associated with methylcrotonylglycinuria (MCG)

Mutation	Location	Structural Observations
MCC α		
BC domain		
Q123H	αF-β4 loop	On the surface, next to the BC-BC interface in the holoenzyme.
I125M	β4	In hydrophobic core. May disrupt structure.
E134K	β4-αG loop	Near the active site. Interacts with the side chain of Arg339, which recognizes the bicarbonate substrate.
M160R	αH-αI loop	In hydrophobic core near the active site.
S187P	β6-αK loop	On the surface. N-terminal cap of helix αK.
R232W	αL-β11 loop	On the surface of the B domain.
A289V	β14	In hydrophobic core. May disrupt the structure.
A291V	β14-αM loop	In hydrophobic core near the active site.
M325R	β15	Strand β15 contains Glu322, a ligand to Mg^{2+}. Also near the base of domain B of BC. May affect the conformational change (open-closed transition) of domain B. Has also been reported to reduce protein level in the cell.
Q372P	αO-β17 loop	Side chain hydrogen-bonded to the main-chain amide and carbonyl of residue 270 (strand β13). May be important for structural integrity.
G379S	β17	Just prior to strand β17.
R385S	β17	Catalytic residue. Stabilizes the biotin enolate.
L437P	β20	In hydrophobic core. May disrupt the structure.
I460M	β21	In hydrophobic core, at the interface with the BT domain.
BT domain		
D532H	Hook (αV-β22 loop)	In the interface with the β subunit. The primary effect is on splicing. The mutation abolishes a 5' splice site, leading to the skipping of an exon.
S535F	Hook (αV-β22 loop)	In the interface with the β subunit.
MCC β		
N domain		
E99Q	β1	Glu99-Arg84 ion pair is located near the interface with the BT domain. May disrupt the holoenzyme.

S101F	β1-β3 loop	Side chain hydrogen-bonded to main-chain carbonyl of residue 528. Bulkier side chain may disrupt structure. Near the interface with the BT domain.
R155Q/W	α3	Buried ion pair with Asp529. May disrupt the structure.
C167R	β6	In hydrophobic core. May disrupt the structure.
S173L	β6	In hydrophobic core, and side chain hydrogen-bonded to main-chain carbonyl of Gly143, which is near the adenine base of CoA. May disrupt the structure and CoA binding.
H190Y/R	β7-α4 loop	Near the β subunit interface and the methylcrotonyl binding site of β subunit. In a cluster with R193C/H and A456V.
R193C/H	α4	In central cavity of β dimer. Ionic interactions with side chain of Glu189, and Asp458 from another subunit.
A218T	β9	Near the methylcrotonyl group and the biotin. May disrupt substrate binding.
H266L	α7	In hydrophobic core.
R268T	α7	On the surface. In the β subunit interface.
D280Y	α8	Interacts with the side chain of Arg86.
H282R	α8	In the surface with the αW helix of the BT domain.
P310R	N-C linker	In linker between N and C domains. Bulkier Arg side chain may disturb structure.
C domain		
V339M	α2-β1 loop	In hydrophobic core. May disrupt the structure. In a cluster with P310R and D340V.
D340V	α2-β1 loop	Interacts with the side chain of Arg538.
V375F	β5	In the interface with the BCCP domain, near the active site of CT. May disrupt BCCP binding to the CT active site.
N403T	β6	Next to the interface with BCCP.
I437V	β8	In hydrophobic core. May disrupt the structure. The primary effect is on splicing. The mutation creates a new 5' splice site, leading to the skipping of part of an exon.
A456V	α5-β10 loop	In hydrophobic core.
K555E	C-terminal loop	On the surface, faces the central cavity of the β_6 hexamer.

References:

[1] Huang, C. S. *et al*. Crystal structure of the a6b6 holoenzyme of propionyl-coenzyme A carboxylase. *Nature* **466**, 1001-1005 (2010).

[2] Kress, D. *et al*. An asymmetric model for Na+-translocating glutaconyl-CoA decarboxylase. *J. Biol. Chem*. **284**, 28401-28409 (2009).

[3] Zhang, H., Yang, Z., Shen, Y. & Tong, L. Crystal structure of the carboxyltransferase domain of acetyl-coenzyme A carboxylase. *Science* **299**, 2064-2067 (2003).

[4] Knowles, J. R. The mechanism of biotin-dependent enzymes. *Ann. Rev. Biochem*. **58**, 195-221 (1989).

[5] Wendt, K. S., Schall, I., Huber, R., Buckel, W. & Jacob, U. Crystal structure of the carboxyltransferase subunit of the bacterial sodium ion pump glutaconyl-coenzyme A decarboxylase. *EMBO J*. **22**, 3493-3502 (2003).

[6] Chou, C.-Y., Yu, L. P. C. & Tong, L. Crystal structure of biotin carboxylase in complex with substrates and implications for its catalytic mechanism. *J. Biol. Chem*. **284**, 11690-11697 (2009).

[7] Baumgartner, M. R. *et al*. The molecular basis of human 3-methylcrotonyl-CoA carboxylase deficiency. *J. Clin. Investig*. **107**, 495-504 (2001).

[8] Shen, Y., Volrath, S. L., Weatherly, S. C., Elich, T. D. & Tong, L. A mechanism for the potent inhibition of eukaryotic acetyl-coenzyme A carboxylase by soraphen A, a macrocyclic polyketide natural product. *Mol. Cell* **16**, 881-891 (2004).

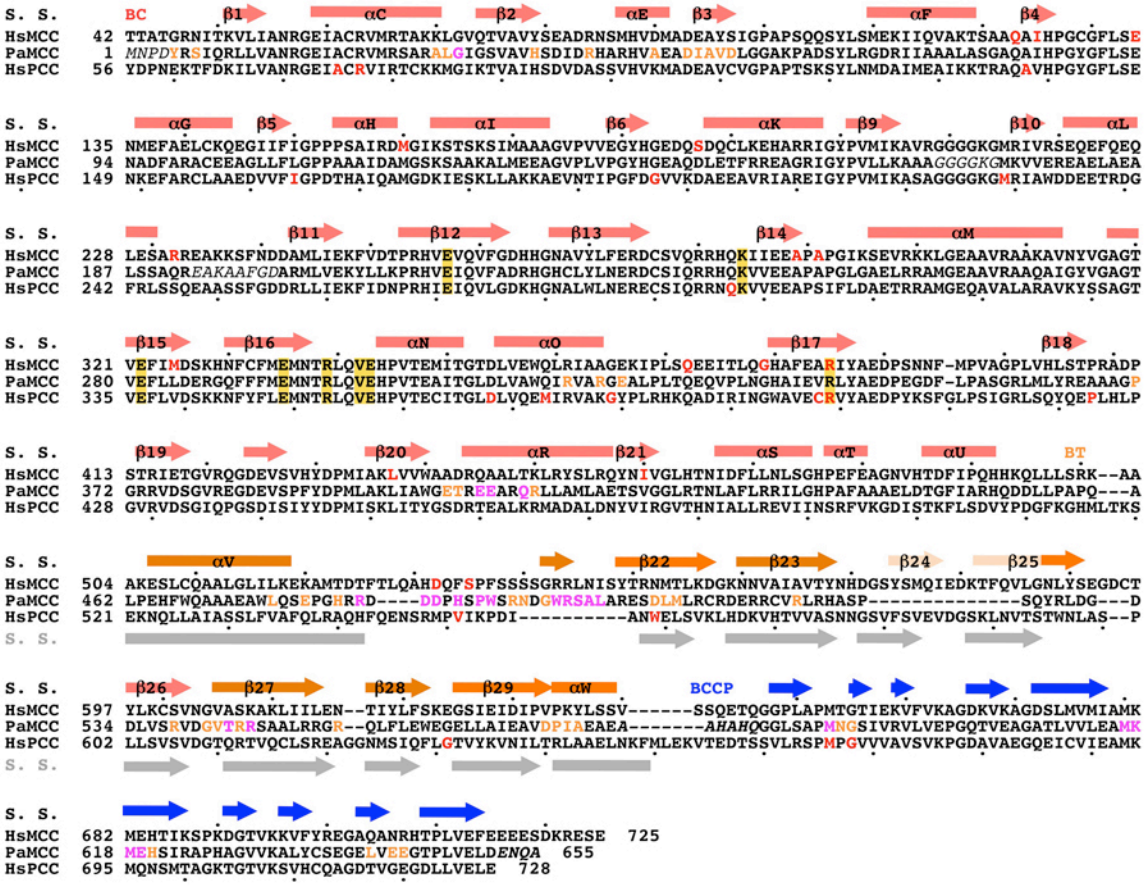

Fig. 1. Sequence alignment of the α subunits of human MCC (HsMCC), *P. aeruginosa* MCC (PaMCC), and human PCC (HsPCC). The BC, BT, and BCCP domains are indicated by the colors of the secondary structure elements (S. S.). Mutation sites associated with methylcrotonylglycinuria (MCG) are shown in red in the HsMCC sequence, and those associated with propionic acidemia (PA) are shown in red in the HsPCC sequence. Residues in the active site are highlighted with the gold background. The colored residues in PaMCC highlight those with >50 Å^2 (magenta) or >15 Å^2 (light brown) buried surface area in the holoenzyme interface. Residues in PaMCC that are not observed in the structure are shown in italics. The dots at the top of the alignment mark every 10th residue in HsMCC, while those at the bottom mark every 10th residue in HsPCC. The secondary structure elements in the BC domain are named after those in the BC domain of yeast ACC [8]. Strand β24 and the first half of β25 of the BT domain are absent in PaMCC, but are predicted in HsMCC. The secondary structure elements in the BT domain of PCC are shown in gray.

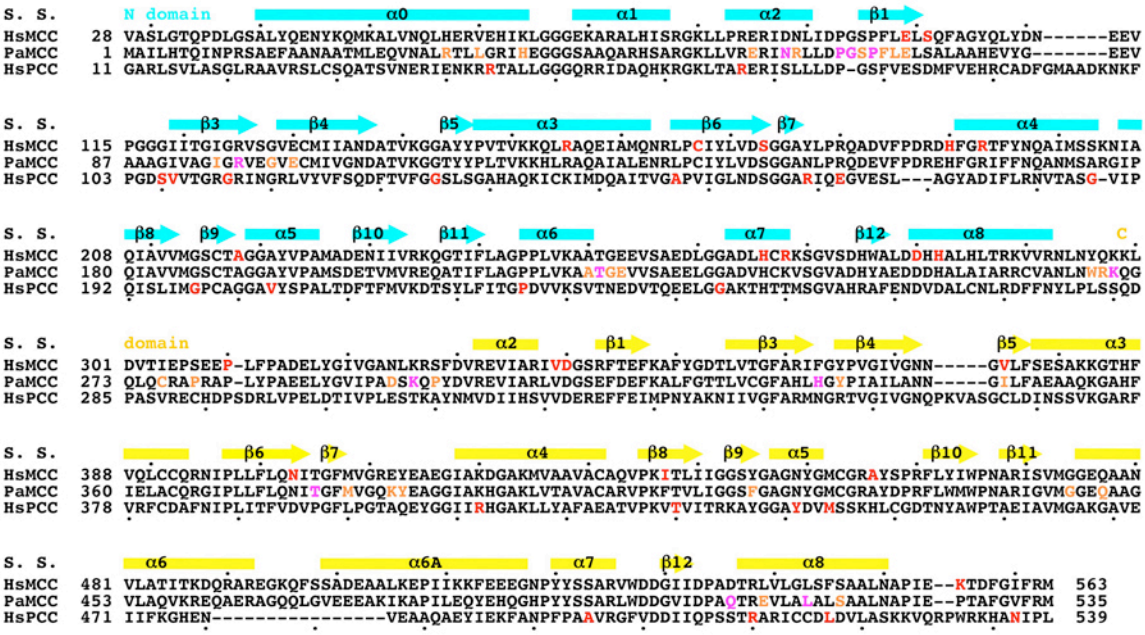

Fig. 2. Sequence alignment of the β subunits of human MCC (HsMCC), *P. aeruginosa* MCC (PaMCC), and human PCC (HsPCC). The N and C domains are indicated by the colors of the secondary structure elements (S. S.). Mutation sites associated with methylcrotonylglycinuria (MCG) and propionic acidemia (PA) are shown in red in the HsMCC and HsPCC sequence, respectively. The colored residues in PaMCC highlight those with >50 $Å^2$ (magenta) or >15 $Å^2$ (light brown) buried surface area in the interface with the α subunit. The dots at the top of the alignment mark every 10^{th} residue in HsMCC, while those at the bottom mark every 10^{th} residue in PaMCC. The secondary structure elements are named after those in the CT domain of yeast ACC [3].

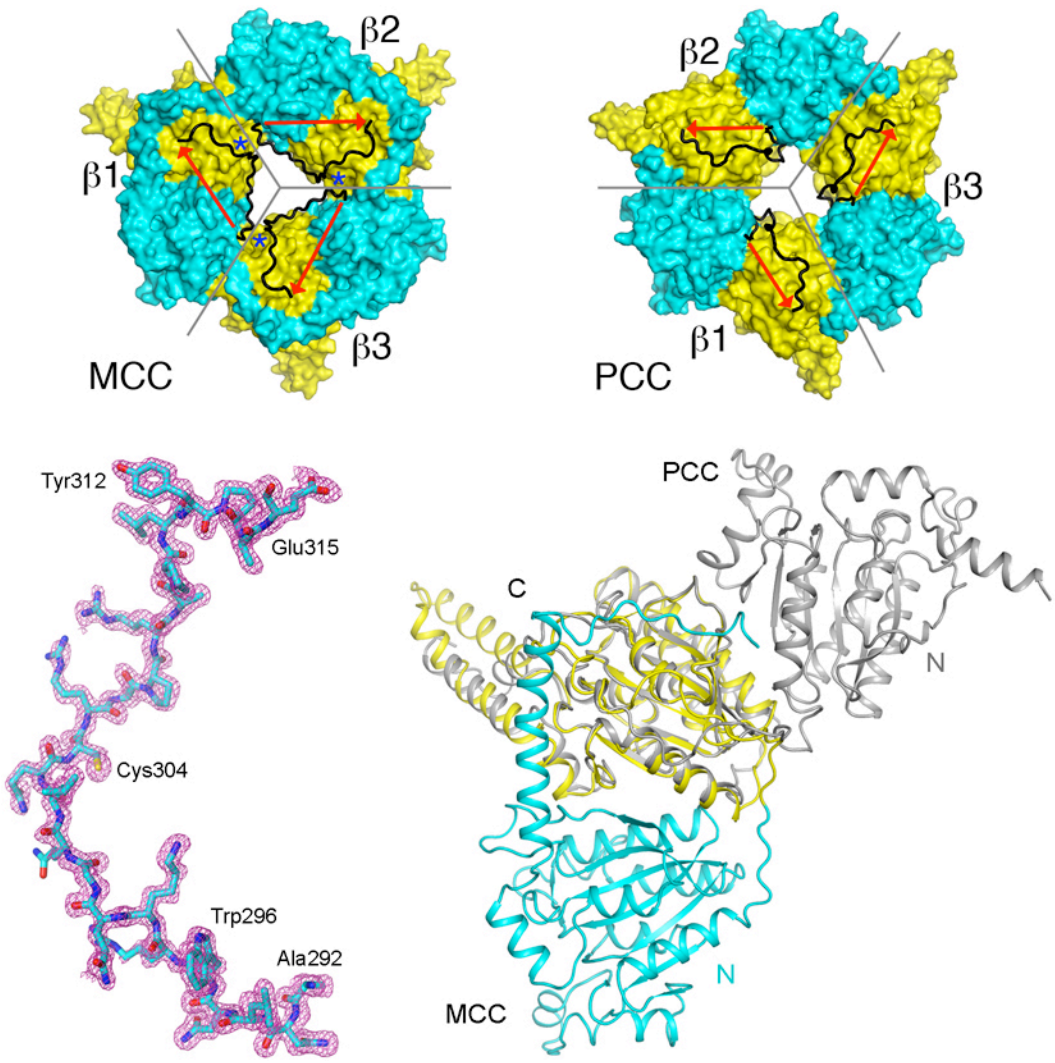

Fig. 3. (***Top***) The linker from the N to the C domains (in black, with the red arrow indicating the direction of linker) runs in opposite directions in MCC (*Left*) and PCC (*Right*) and connects to different C domains, leading to the swapping of the positions of the N and C domains in each subunit between the two enzymes. The two neighboring linkers approach each other closely at one point (blue star) in PaMCC, and a change in connectivity at that position will lead to the PCC organization. The boundaries of each subunit are indicated by the gray lines. (***Bottom left***) Omit F_o–F_c electron density for the linker in PaMCC at 1.5 Å resolution, contoured at 3σ. (***Bottom right***) Overlay of the structures of the β subunit of PaMCC (in color) and PCC (gray). The C domains of the two structures are superimposed, but their N domains are in different positions due to the swap. All structure figures were produced with the program PyMOL (www.pymol.org).

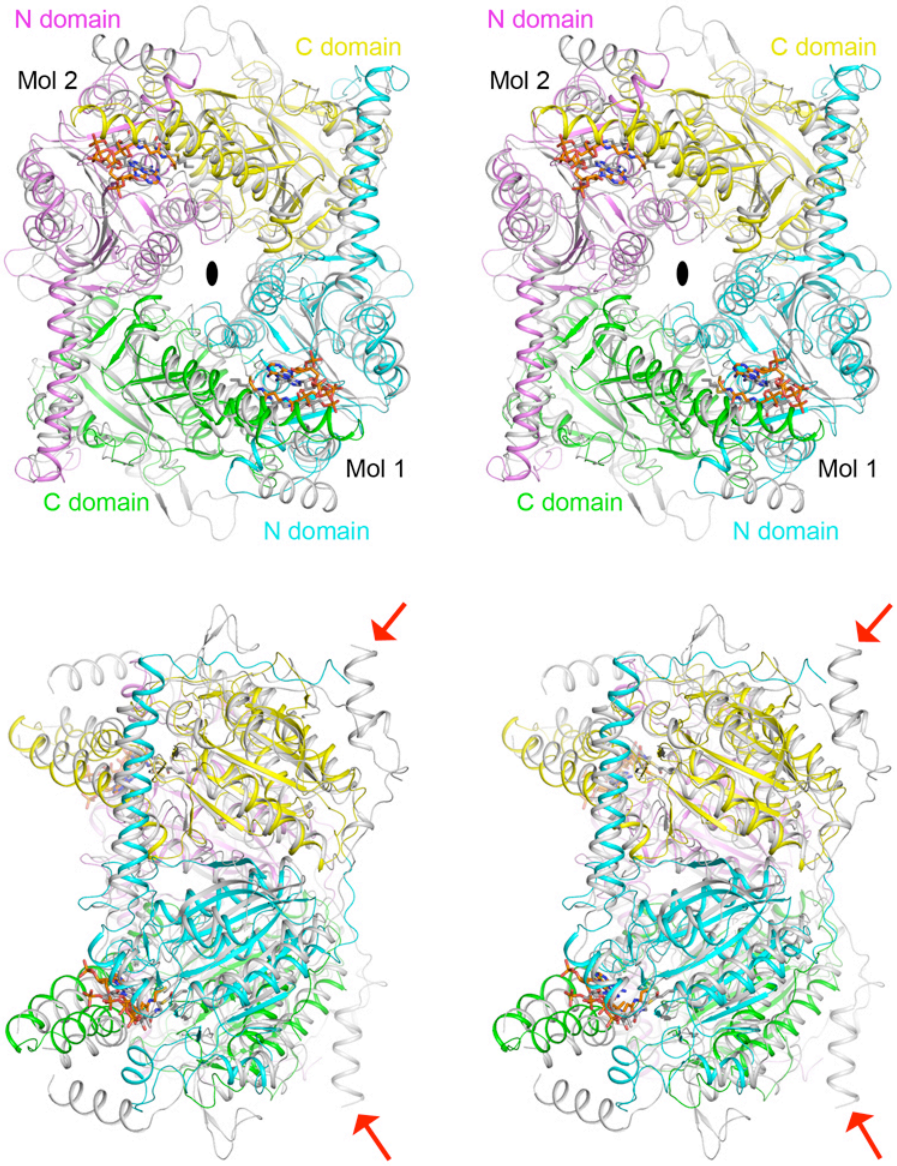

Fig. 4. (***Top***) Stereo drawing of the overlay of a β_2 dimer of PaMCC holoenzyme in complex with CoA (in color) with the GCDα dimer in complex with crotonyl-CoA (in gray) [2]. The N and C domains are labeled, and the two-fold axis of the dimer is indicated by the oval in black. (***Bottom***) The same overlay after a 90° rotation around the vertical axis. The C-terminal helices of the two GCDα monomers are indicated with the red arrows. These helices clash with other monomers in the hexamer interface of PaMCCβ, which is one of the reasons why GCDα cannot form a similar hexamer. It is also possible that residues at the hexamer interface have been mutated to disfavor that oligomer for GCDα. Instead, GCDα dimer can form a tetramer using a different interface [2].

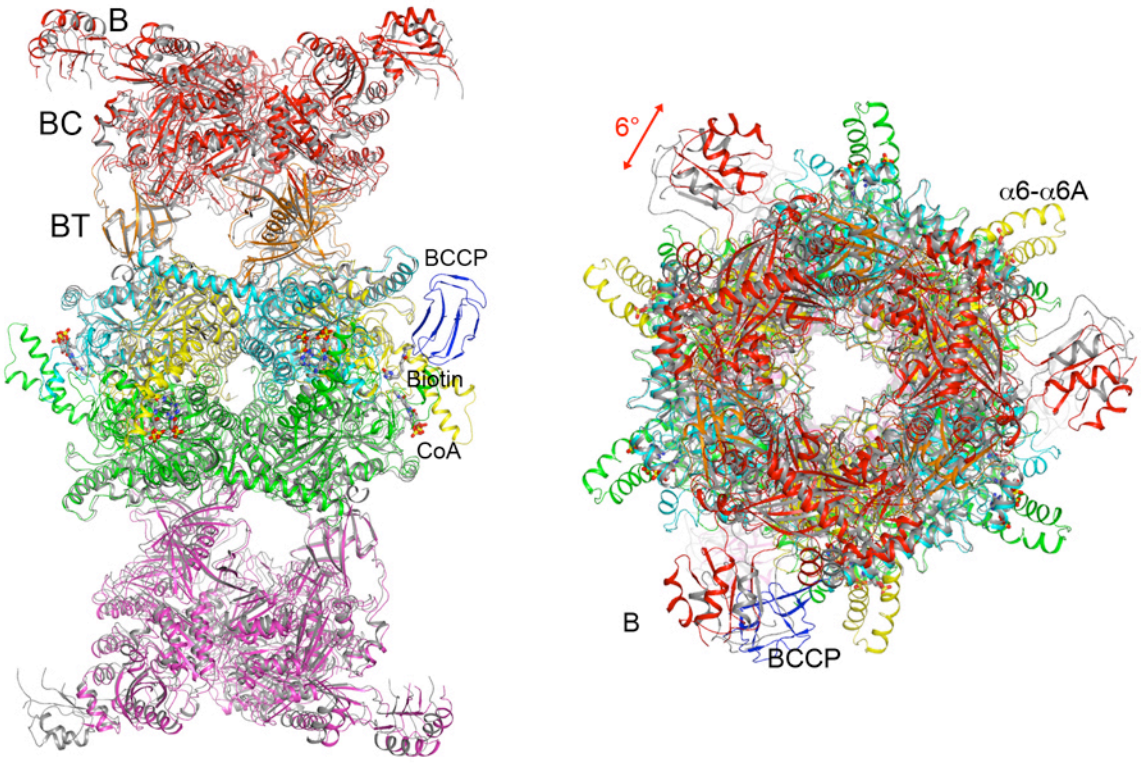

Fig. 5. Overlay of the structures of the CoA complex (in color) and the free enzyme (gray) of PaMCC holoenzyme. (***Left***). Viewed down a two-fold axis of the dodecamer. (***Right***). Viewed down the three-fold axis. The 6° rotation in the α subunits of the two structures are indicated in red. The BCCP domain, α6-α6A protrusion, as well as several other segments near the active site of the β subunit, are disordered in the free enzyme.

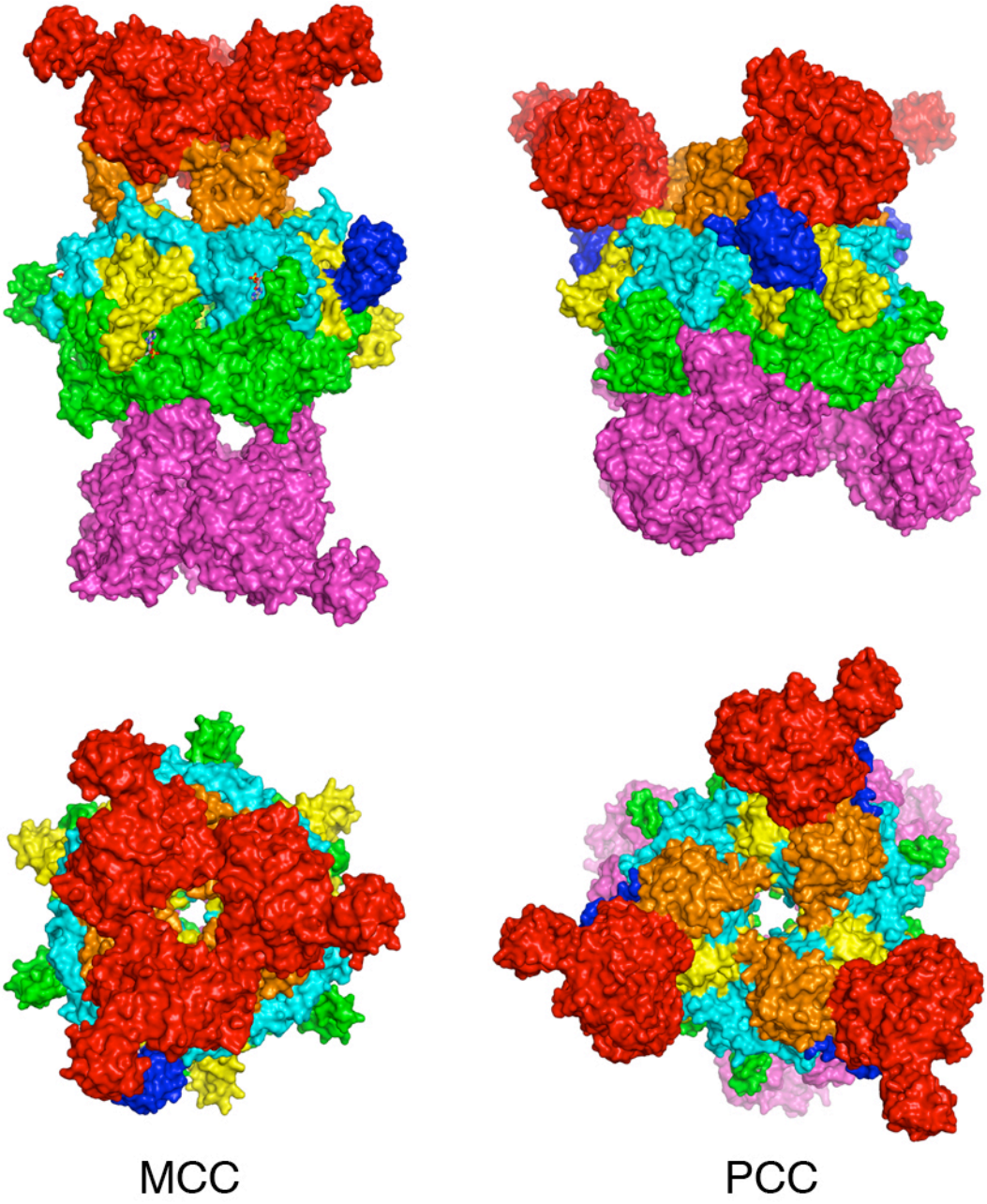

Fig. 6. (***Left***). Side and top views of the PaMCC holoenzyme molecular surface. (***Right***). Side and top views of the PCC holoenzyme, showing dramatic differences in the overall architecture of the two enzymes.

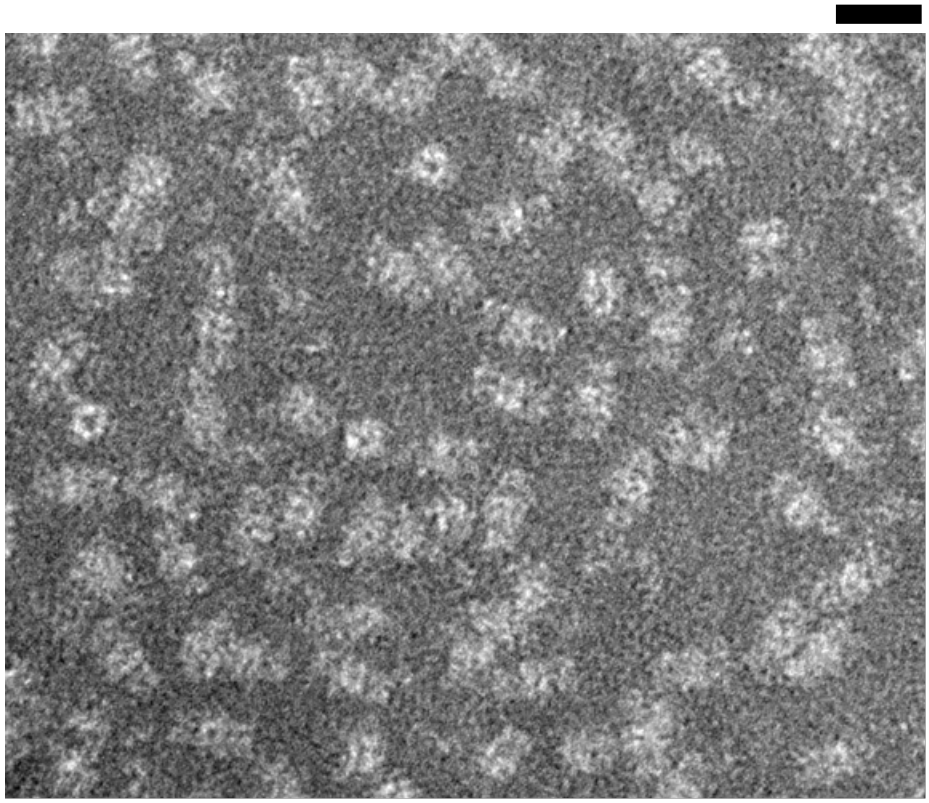

Fig. 7. Transmission electron micrograph of negatively stained PaMCC. Scale bar = 200 Å.

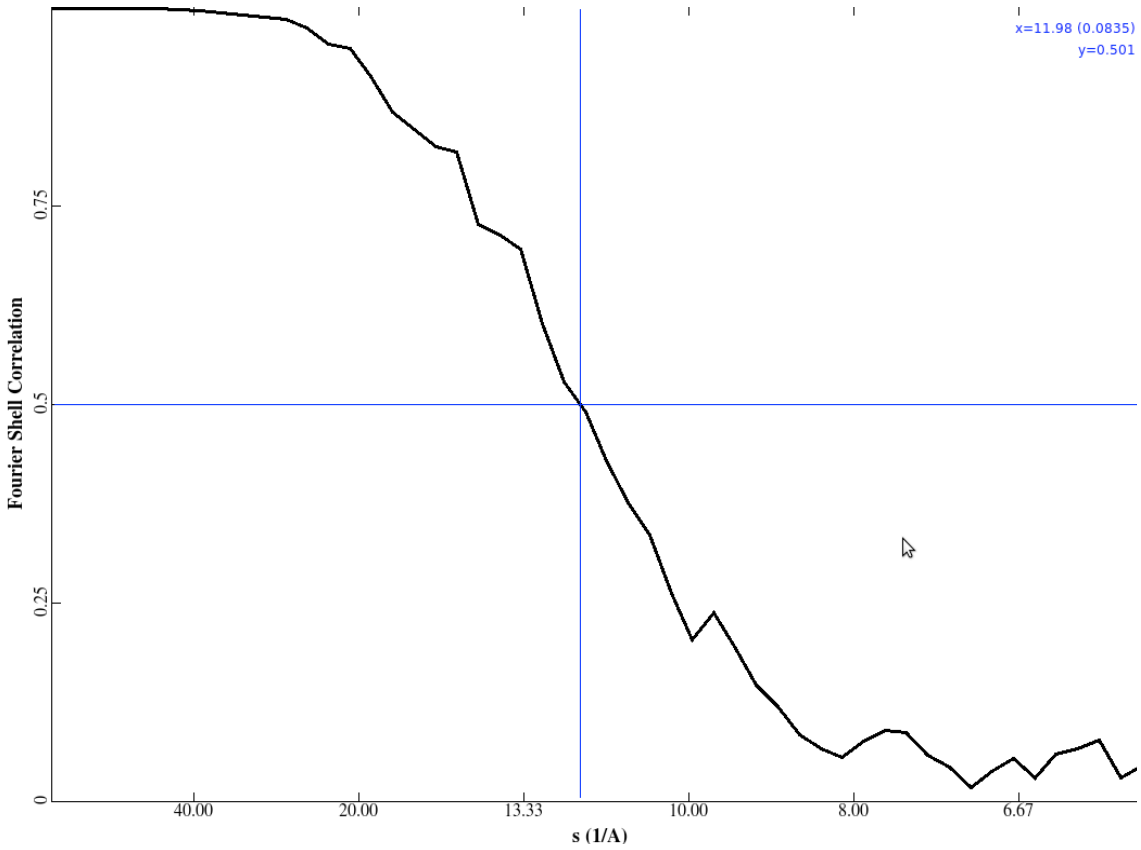

Fig. 8. Resolution assessment based on Fourier shell correlation (FSC). The FSC coefficients between the two reconstructions each from half of the full data sets during the last four refinement rounds are plotted as a function of spatial frequency (1/Å). Using the FSC = 0.5 criterion, the resolution of the final reconstruction is about 12 Å.

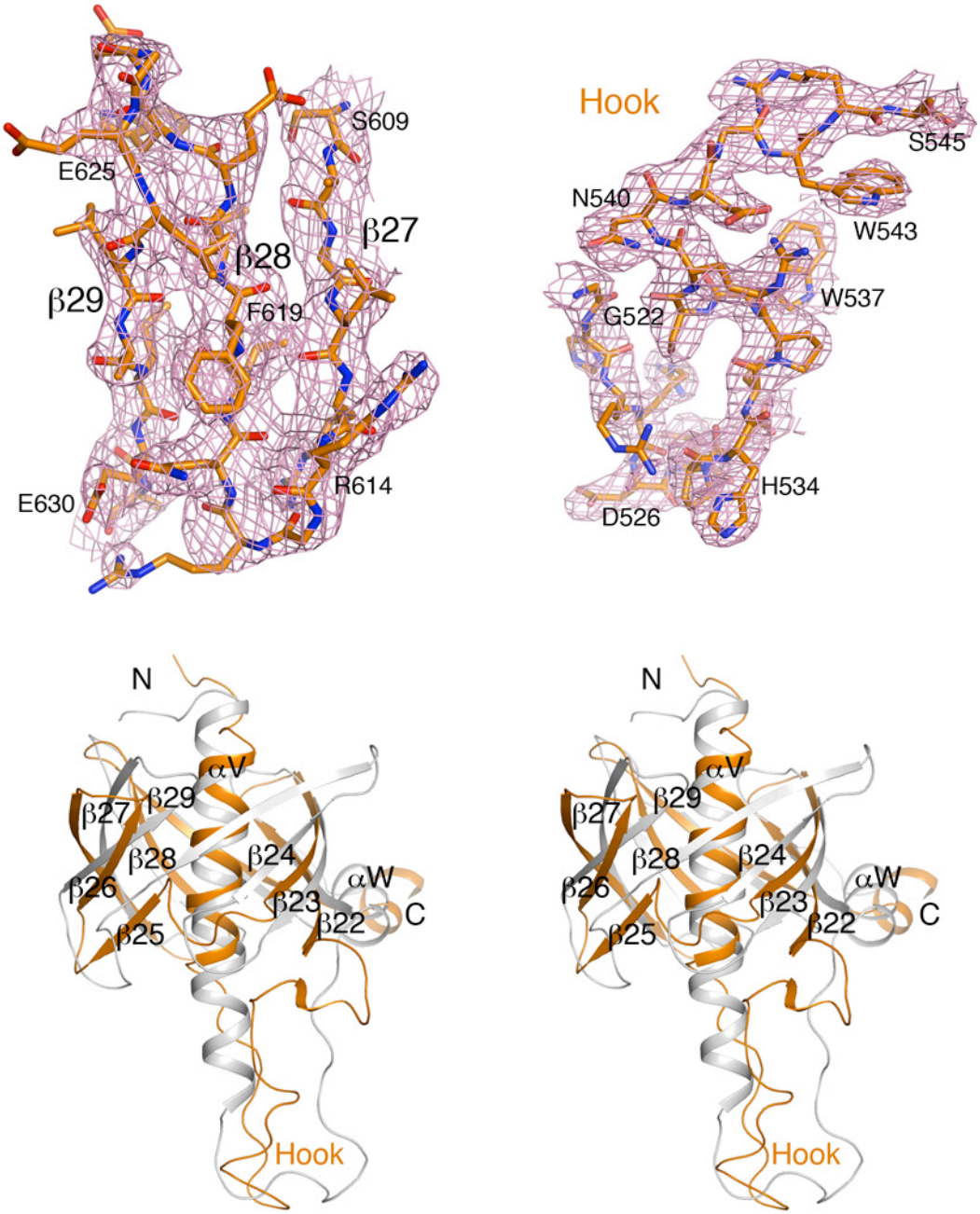

Fig. 9. (***Top***) Simulated annealing omit F_o–F_c electron density map at 2.9 Å resolution for strands β27-β29 (residues 609-631, *Left*) and the hook (residues 522-545, *Right*) in the BT domain of the α subunit. The contour level is at 3σ. (***Bottom***) Schematic drawing in stereo of the overlay of the BT domain of PaMCC (orange) with that of PCC (gray).

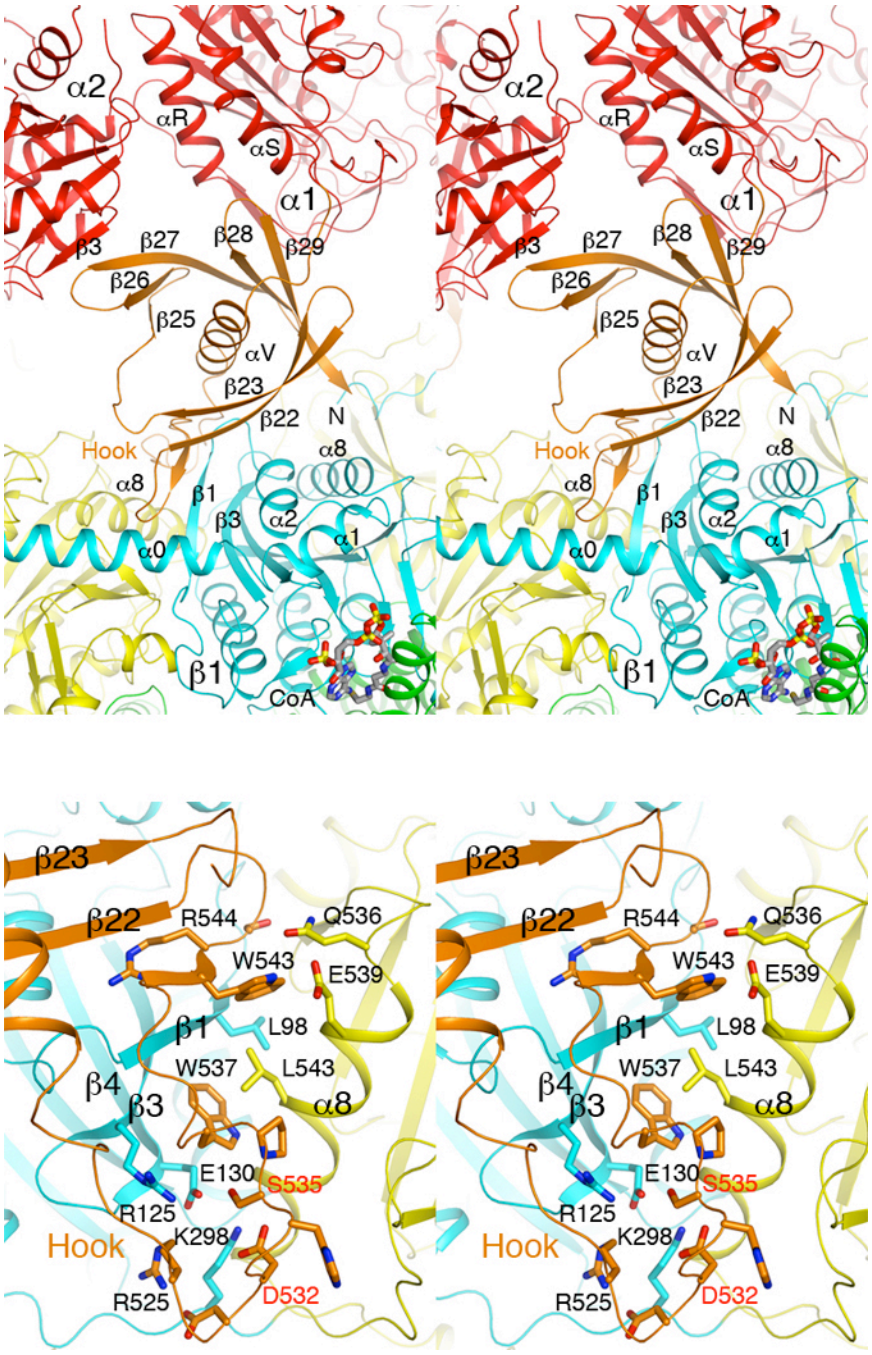

Fig. 10. (***Top***) Schematic drawing in stereo of the interactions of the BT domain (orange) in the PaMCC holoenzyme. (***Bottom***) Schematic drawing in stereo of the interactions between the hook of the BT domain (orange) and the N (cyan) and C (yellow) domains of the β subunit.

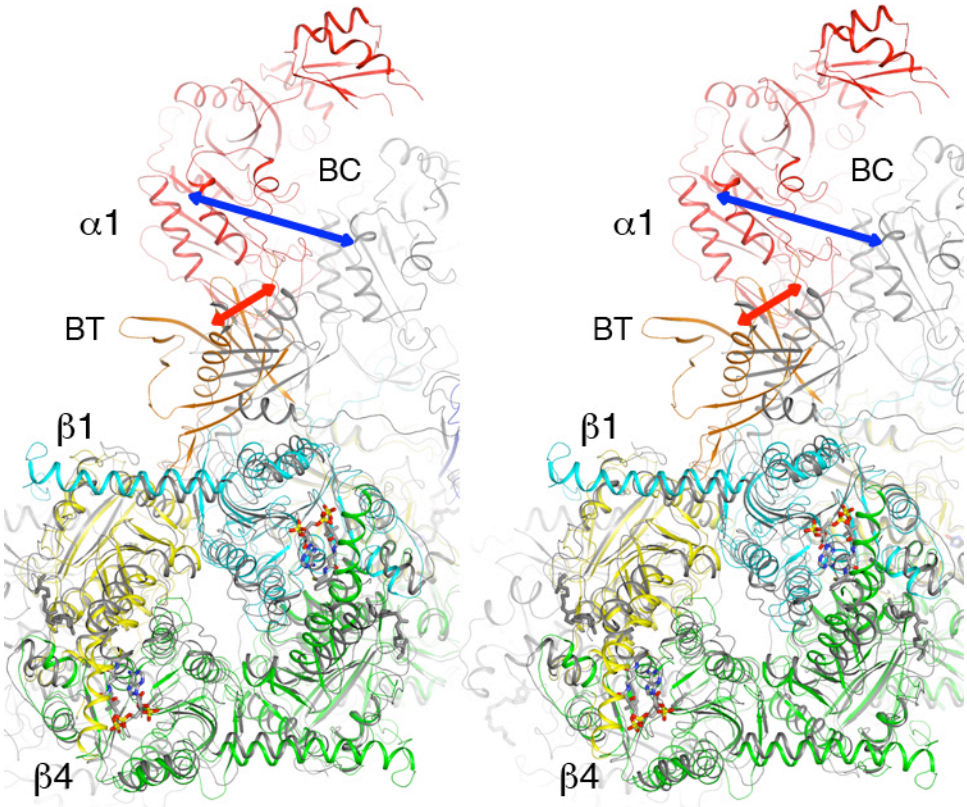

Fig. 11. The positions of the BT domain relative to the β subunit are different in PaMCC and PCC. The PCC holoenzyme structure is rotated by 60° around the 3-fold axis (the pseudo symmetry of the hexamer), which brings its β hexamer (in gray) into overlay with that of MCC (in color). A distinct position of the BT domain in PaMCC (orange) is observed relative to that in PCC (gray, indicated with the red arrow). An independent change in the positions of the BC domains is also apparent (indicated with the blue arrow).

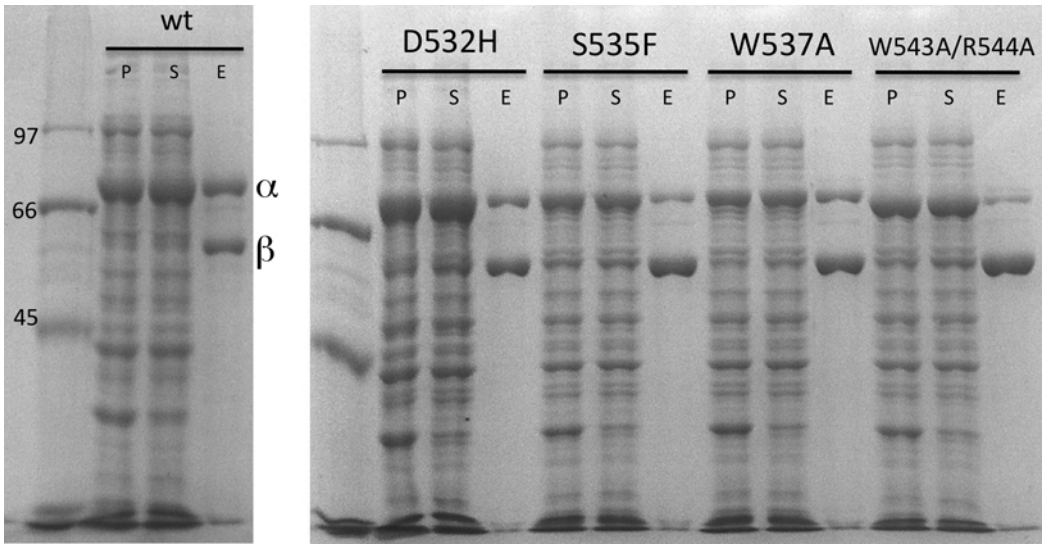

Fig. 12. Mutations in the hook of the BT domain can destabilize the MCC holoenzyme. Mutations were introduced in the hook of PaMCC based on the structural information, and the effects of the mutation on the formation of the holoenzyme were examined by nickel pulldown experiments after bacterial expression with SDS-PAGE. The β subunit carried a His tag, and therefore the elution (E) from a nickel column, compared to the total amount of over-expressed protein in the pellet (P) and soluble (S) fractions, gave an indication of the stability of the holoenzyme. For example, the eluate for the W543A/R544A double mutant contained a large excess of the β subunit, even though the α subunit was soluble, suggesting that the holoenzyme has been destabilized by this mutation. The D532H mutation also had some effect, even though this disease-causing mutation primarily affects splicing in humans. It should also be noted that this assay is under over-expression conditions. Under physiological conditions, where the concentrations of the two subunits are likely much lower, the effect of the mutations on the stability of the holoenzyme may be more pronounced.

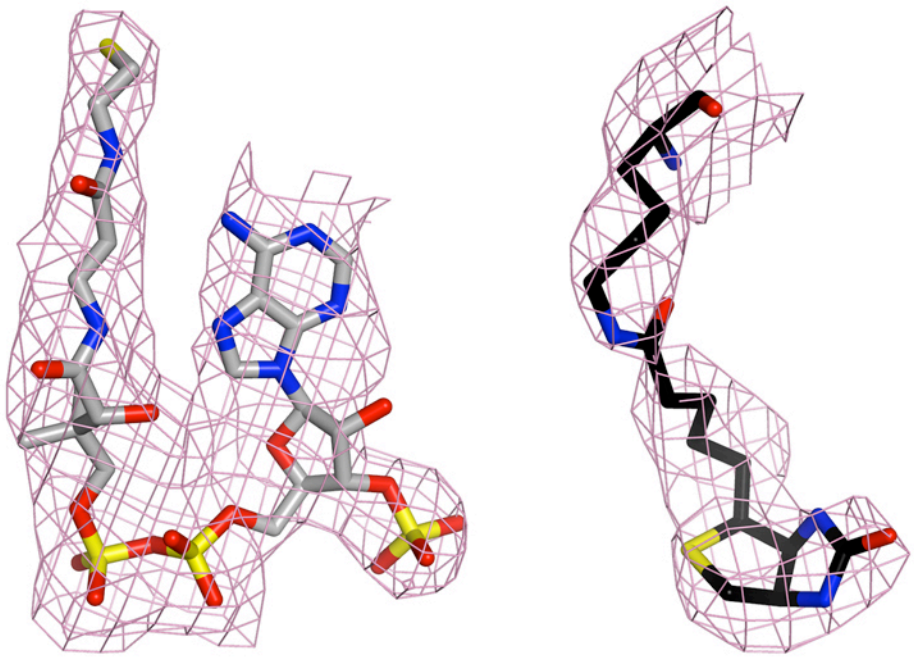

Fig. 13. Simulated annealing omit F_o–F_c electron density map at 3.5 Å resolution for CoA (***Left***) and residue Lys681 with its attached biotin (***Right***). The contour level is at 3σ.

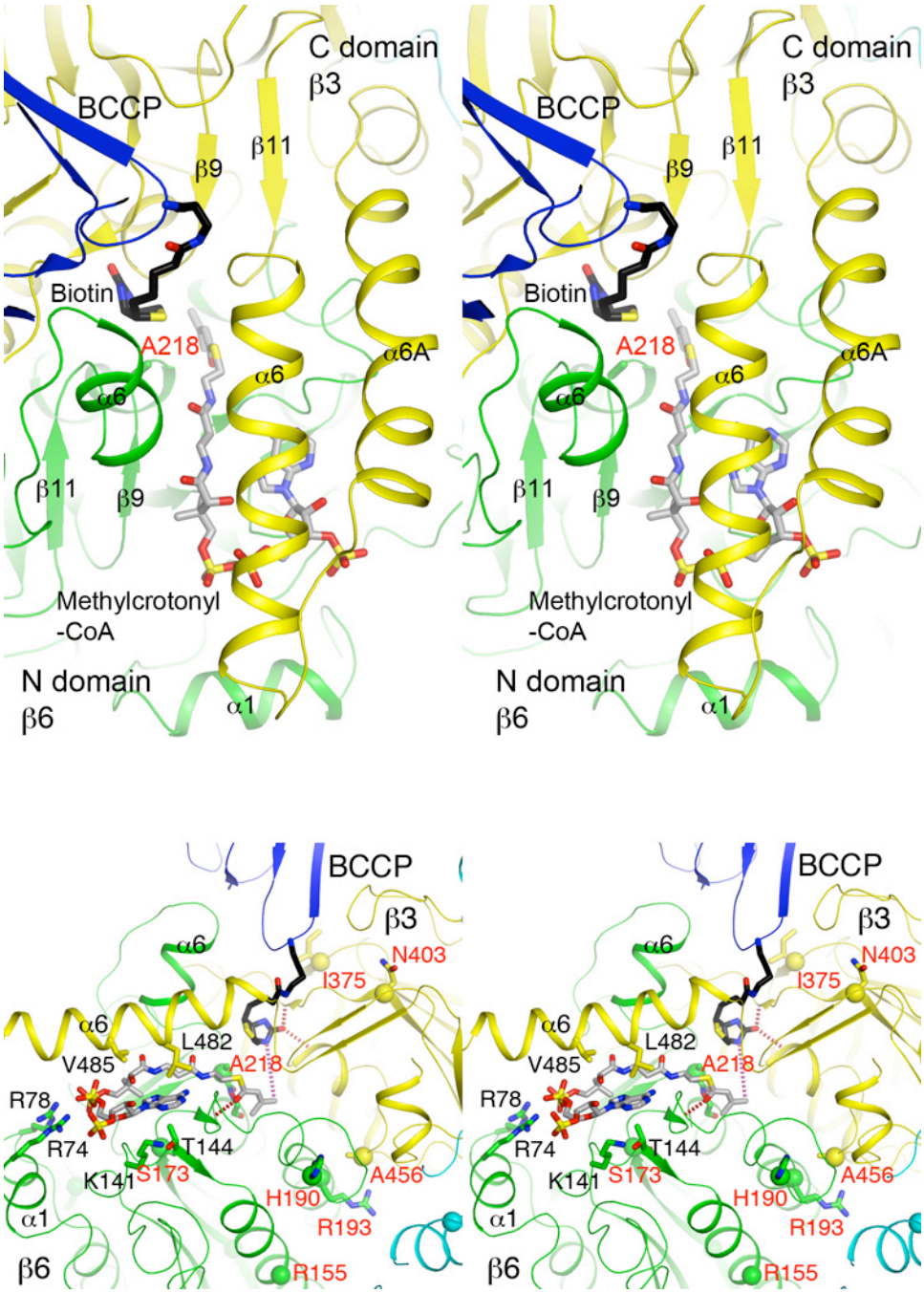

Fig. 14. (***Top***) Schematic drawing of the active site of the β subunit. The modeled position of methylcrotonyl-CoA is shown. (***Bottom***) The active site of the β subunit, viewed from the right of the top panel. Disease causing mutations are shown with a sphere for the Cα atom and labeled in red. Interactions in the two oxyanion holes are indicated with the dashed lines. The N1' atom of biotin and the reactive γ carbon of methylcrotonyl-CoA are also linked by a dashed line. Residues in helix α6A are omitted for clarity.

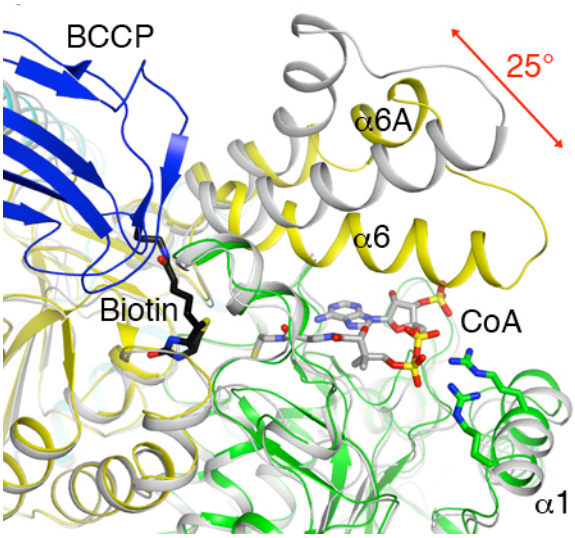

Fig. 15. A large conformational change for helices α6 and α6A in the CoA complex (in color) as compared to the structure of PaMCCβ alone (in gray). The 25° rotation is indicated with the red arrow. A smaller conformational change is also observed for helix α1.

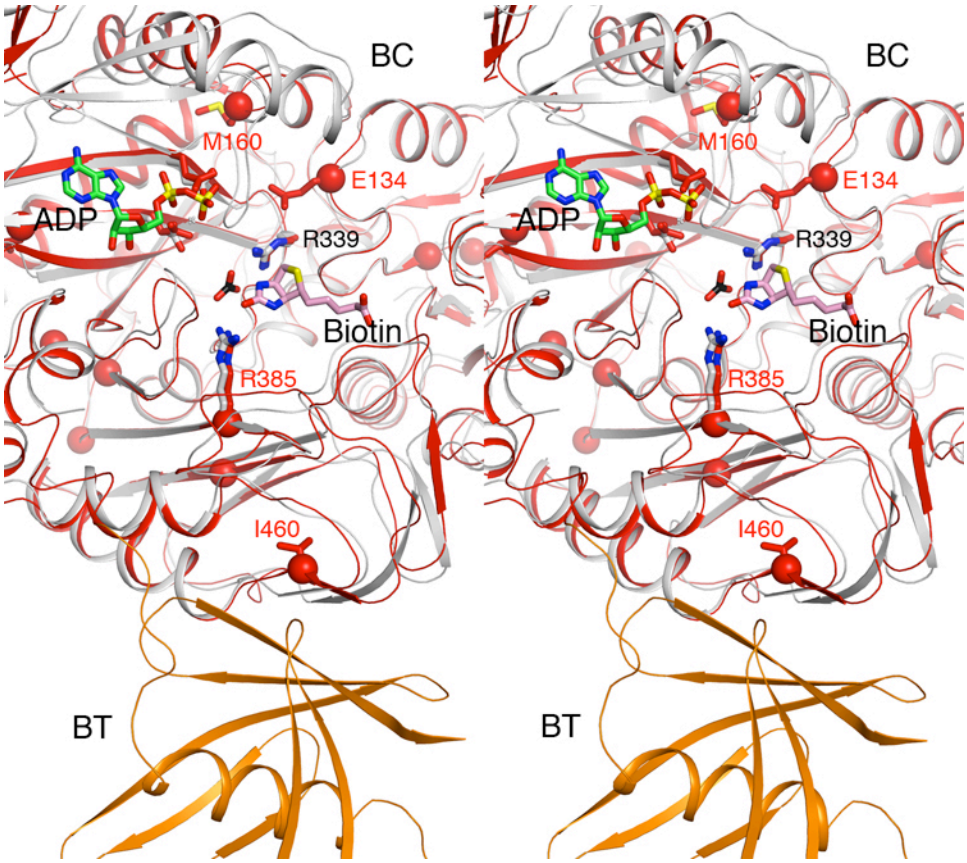

Fig. 16. Disease-causing mutations near the BC active site of MCC. The structure of *E. coli* BC [6] is shown in gray, and its bound ADP (in green), bicarbonate (black) and biotin (pink) are also shown. Disease causing mutations are shown with a sphere for the Cα atom and labeled in red.

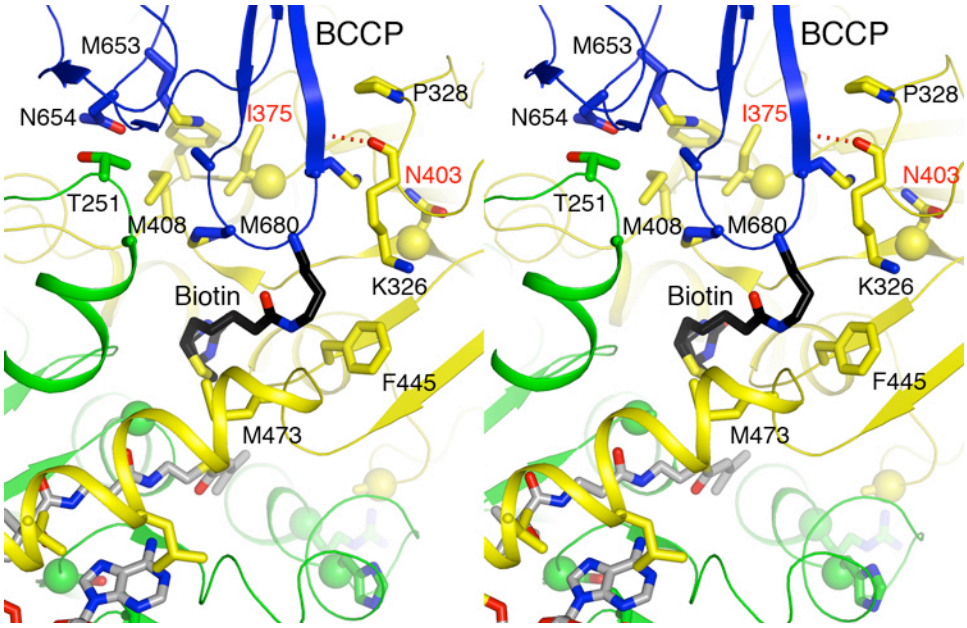

Fig. 17. Interactions between BCCP and the β subunits in PaMCC. Disease causing mutation sites in HsMCC are labeled in red.

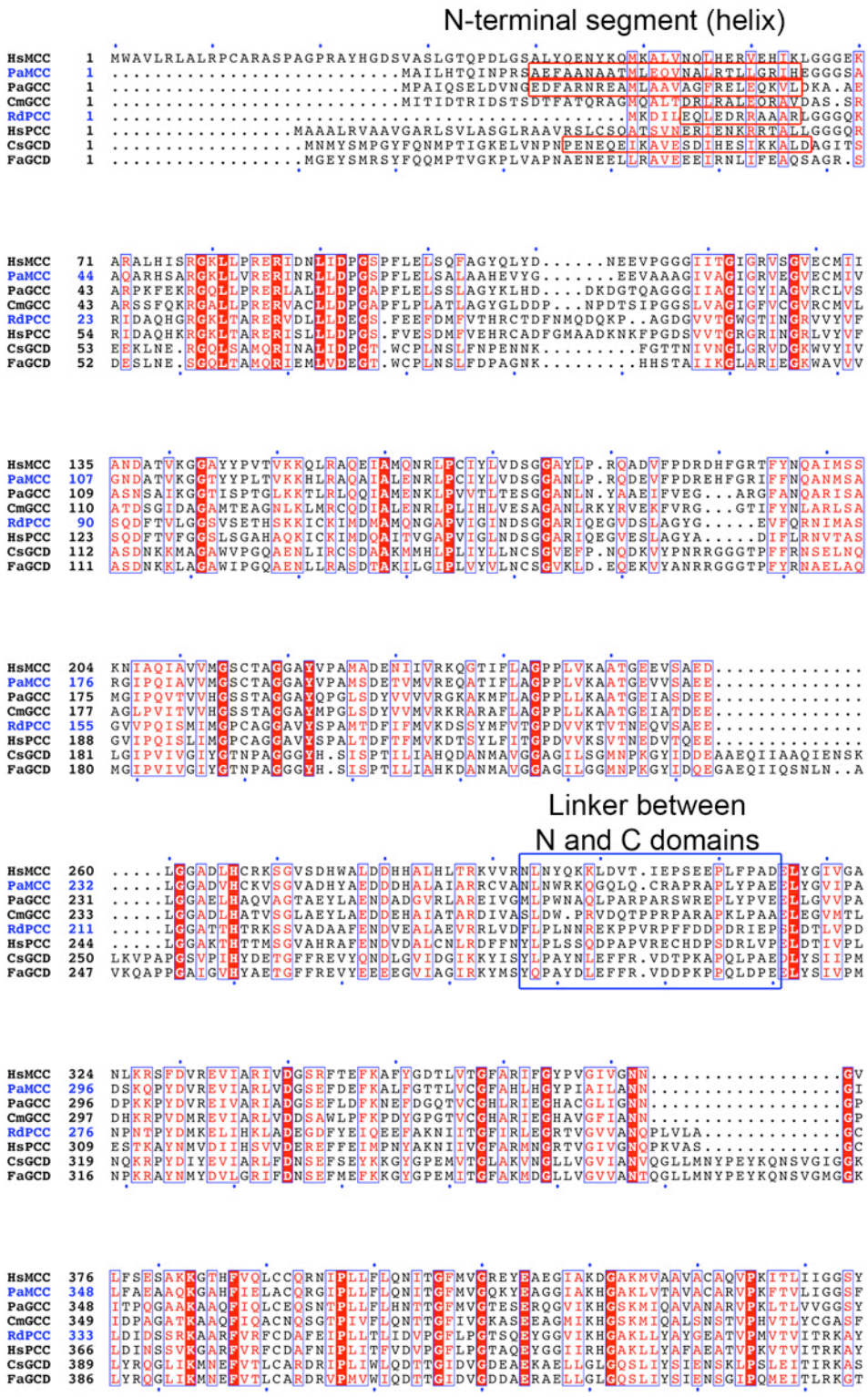

Fig. 18 (continued on next page)

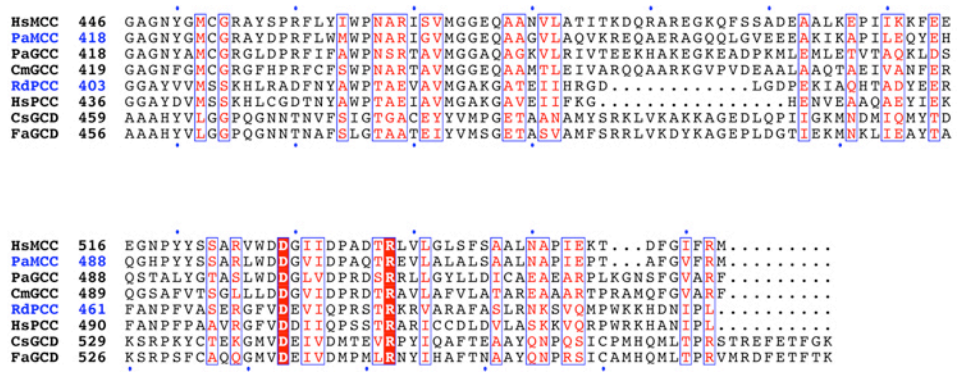

Fig. 18. Sequence alignment of the β subunits of human MCC (HsMCC) and PCC (HsPCC), *P. aeruginosa* MCC (PaMCC) and GCC (PaGCC), *Cupriavidus metallidurans* GCC (CmGCC), *Roseobacter denitrificans* PCC (RdPCC), and the α subunits of *Clostridium symbiosum* GCD (CsGCD), and *Filifactor alocis* GCD (FaGCD). The helix at the N-terminus as observed in the crystal structures of PaMCC, RdPCC and CsGCD are shown in red boxes. A similar helix is expected in PaGCC based on secondary structure predictions. MCC, GCC and GCD also contain a loop at the N-terminus in addition to the long helix. In contrast, the N-terminal segment and helix of RdPCC is much shorter. For HsMCC and HsPCC, the first ~30 residues belong to the mitochondrial targeting sequence and are not in the mature protein.

The linker between the N and C domains of these enzymes is boxed in blue. It is roughly the same length, but is poorly conserved.